

Compact Shortened V-Band Conical Dielectric Core Horns Corrected by Lenses



Key Points:

- We use the axisymmetric character of conical horns and some lenses to employ higher-order curved hybrid finite elements
- Projecting the problem to a bidimensional mesh, the computational time is drastically reduced and the optimization of the device results much more efficient
- Following this approach, we obtain a procedure to reduce the size of very long antennas by adding double convex lenses and dielectric cores; ultra-shortened horns, of a size as small as one wavelength, can then be achieved

J. M. Gil¹ 

¹Signals, Systems and Radio Communications Department, Information Processing and Telecommunication Center, Universidad Politécnica de Madrid, Madrid, Spain

Correspondence to:

J. M. Gil,
josemaria.gil@upm.es

Citation:

Gil, J. M. (2022). Compact shortened V-band conical dielectric core horns corrected by lenses. *Radio Science*, 57, e2022RS007618. <https://doi.org/10.1029/2022RS007618>

Received 17 OCT 2022
Accepted 24 OCT 2022

Abstract A procedure of designing ultra-short conical horns corrected by lenses, is boarded at this work. The method takes advantages of the axisymmetric character of the conical horns to project the problem to a bidimensional mesh, reducing the computational time and making easy the optimization of the device. This approach is not used for most popular commercial codes which employ a 3D analysis of the whole antenna. Horn antennas exhibit some remarkable radiation characteristics as they are high directivity, low crosspolar level and symmetric patterns with low return losses on a reasonable bandwidth. The price to pay is handle devices very long and weighed, so it is demanding to find lines of design to shorten and make compact horns to be incorporated to the current communication systems. In this work, we show the advantages to use a double convex lens together with a dielectric core, added to the horn, to achieve a compact and shortened horn maintaining a good performance. Conical horns, of a size as small as one wavelength, can be achieved. To reach such shortening, a double convex lens and a dielectric core must be added to the antenna. The parameters of the final prototype, at 60 GHz, are the following: Length: $\approx \lambda$, Directivity = 20 dBi, Cross polar Peak = -19.1 dB, Beam width on copular plane = 18.3° , Side Lobe Levels lower than -20 dB (both H and E plane), Return losses = -30.7 dB, and presenting an smooth frequency behavior on a wide bandwidth.

1. Introduction

The design of small compact conical horns, at millimeter wavelengths, has reached a relevant increase at the last years. Ultra-high speed communication systems for wireless multimedia applications demand the design of compact and cheap antennas to link the transceivers in the network. Many antenna systems have been presented to deal with these goals as on-chip antennas (M. Alibakhshikenari et al., 2022), and antennas making use of artificial materials (M. Alibakhshikenari, et al., 2020). Conical horns could be good candidates to be incorporated to these systems. However, their size and length make not recommendable for the integrations in such systems. The shortening of the horns deteriorates the phase diagram at the aperture, but the use of dielectric cores and lenses can compensate the worsening of the performance of the antenna. On the other hand, the increase of the weight due to the presence of the dielectric core and/or lenses becomes acceptable for many applications at these frequencies. In this subject, several authors have published some studies about shortened conical horns, lens-corrected, with or without dielectric core (M. K. T. Al-Nuaimi et al., 2014; E. L. Holzman, 2004; M. Shaik & Rama, 2013; A. Rolland et al., 2010; D. Wu, et al., 2015; S. Zhang et al., 2018) or meta-horns (K. Liu et al., 2019; D. Ramaccia et al., 2013); our intention in this work is to add some new results to these lines of computer-aided design.

The widespread incoming of communication systems at 60 GHz demands inexpensive and straightforward manufacture of antennas that copes well with shortened lens-corrected horns. The use of additive techniques of manufacture, like 3D printing and the metalization of the external dielectric layer constitutes an interesting option to get components at these frequencies.

At the present work, we use a technique based on finite elements applied to bodies of revolution (BoR-FEM), by closing the problem by means of an expansion of spherical modes (SM) surrounding the antenna (BoR-FEM-SM). This approach has been used for our group for many years due to its reliability and robustness in complex problems (J. M. Gil et al., 2006, José Martínez-Fernández et al., 2007). We present here some new results for wide flare angle shortened conical horns, and ultra-shortened conical horns focused by both, simple and double convex lenses. First, in Section 3, we optimize a 90° flare angle loaded with a hyperbolic dielectric lens (convex-plane lens) by adding a second lens (double-convex lens) and optimizing the value of the permittivity of the material and the thickness of the lens; then, we obtain an antenna with a better performance. Second, in Section 4, we address

© 2022. The Authors.

This is an open access article under the terms of the Creative Commons Attribution-NonCommercial-NoDerivs License, which permits use and distribution in any medium, provided the original work is properly cited, the use is non-commercial and no modifications or adaptations are made.

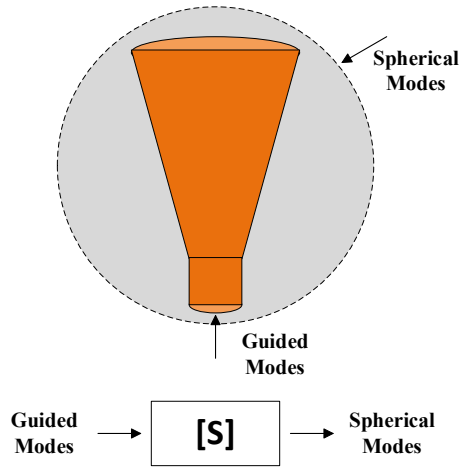


Figure 1. Antenna based on B.O.R. characterized as a two ports circuit: Port 1: circular waveguide; Port 2: Spherical waveguide.

closing the radiator defines a boundary where a spherical mode expansion of the fields is used. The discretization of such kind of problems copes well with 2.5D finite elements. At the port 1, we model the electromagnetic fields by means of analytical modes at the circular waveguide and, at the port 2, we model the radiated fields as an expansion of SM. We must take enough modes to represent adequately the field at the ports and mesh the complete FEM domain, including the sphere, with a sufficient number of degrees of freedom. The spherical surface defines a computational domain for the radiating region. This region may be reduced assuming that the sphere intercepts the conical surface of the horn far enough from the aperture to have negligible fields (and currents) along the interception surface. The optimal radius of the spherical port is decided after a previous study of convergence. It must be noticed that the mesh is bi-dimensional although we need the three field components. The numerical problem is then bi-dimensional and the computation time for a full-wave analysis of the antenna results insignificant, a few seconds in a personal laptop. A brief description of the formulation of the method is described in the following.

the shortening of the same horn in order to get a very compact and small antenna for this frequency band by incorporating a dielectric core together with a double-convex lens. Again, the permittivity and thickness of the lens are optimized and we achieve a prototype of a size slightly longer than one wavelength, and an outstanding performance relative to the radiation behavior and matching to the feeder. Moreover, a study in frequency is carried out showing a stable behavior along a wide band. Radiation patterns are also shown at three frequencies exhibiting a reasonable stability. The prototype may be decomposed into segments that can easily be manufactured by using additive techniques. The materials used in the lens and/or dielectric cores can also be obtained by adding air inclusions in a dielectric commercial material. We have not finished the manufacturing of the prototypes although we hope to reach the capacity to do it in the next future.

2. Formulation of 2.5 D BoR-FEM-SM Problems

The antenna is characterized as a closed circuit. We surround the device by a sphere and we consider the antenna as a two-ports circuit (see Figure 1); a port simulates the input waveguide (feeder) and a second spherical port

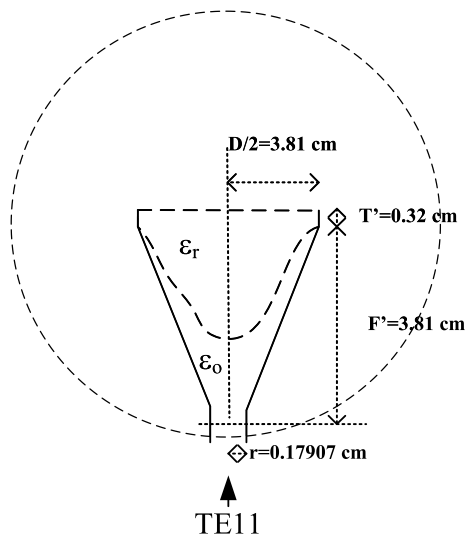


Figure 2. Geometric dimensions of a 45° flare angle conical horn loaded with a convex-plane lens.

The electromagnetic fields in the computational domain are expanded as a series of axisymmetric modes expressed as

$$\vec{H} = \sum_{m=0}^{m=\infty} \left[\vec{H}_r(r, z) \sin m\varphi + \frac{1}{r} H_\varphi(r, z) \cos m\varphi \hat{\varphi} \right] \quad (1)$$

The modes are split up into φ -independent modes ($m = 0$), TE_{0ld} and TM_{0ld} , and hybrid modes with φ -dependence ($m \geq 0$), HE_{mld} . We span the field considering two components, transverse or meridian (r, z), and azimuthal (φ). A curve quadratic tangential vector element is used for the transverse component, and a quadratic Lagrange scalar nodal element for the azimuthal component.

After applying the Galerkin method to the wave equation for the magnetic field H , we get the following equation

$$\int_V (\nabla \times W \cdot [\epsilon_r]^{-1} \cdot \nabla \times H - k^2 W \cdot [\mu_r] \cdot H) dV = \int_{S_p} W \cdot (n_p \times e_{ij}^p) dS_p \quad (2)$$

being W , the test functions, $[\epsilon_r]$, $[\mu_r]$ are the complex permittivity and permeability tensors of the material and n_p is a normal vector inwards the region in each port.

Table 1
Performance of a Shorted Corrected-Lens Conical Horn

f (GHz)	58.6 [3]	62.1 [3]	58.6 [current]	62.1 [current]
Mod(S11)	-17	-12	-18.9	-11.8
D(dB)	26.6	27.1	24.1	25
BWE-Plane	5.9	5.6	7.8	5.5
BWH-Plane	10.1	9.3	11.1	7.2

The expansion of the tangential electric field in the ports, in terms of voltage coefficients, is

$$\mathbf{E}_t^p = \sum_{j=1}^{\infty} V_j^p (v_p) \mathbf{e}_{ij}^p (\xi_p, \varphi_p) \quad (3)$$

(ξ_p, φ_p, v_p) are local coordinates related to each port. Once the problem is discretized by 2D finite elements, a system of equations is obtained

$$[\mathbf{K} - k^2 \mathbf{M}] \{\mathbf{H}_c\} = j\omega\epsilon_0 \mathbf{B}\{\mathbf{V}\}. \quad (4)$$

\mathbf{K} and \mathbf{M} are stiffness and mass sparse matrices, $\{\mathbf{V}\}$ are voltage coefficients, $\{\mathbf{H}_c\}$ are the N_d degrees of freedom of the finite elements approximation. \mathbf{B} is a matrix with the number of modes used at the ports. After a normalization process, the full-wave Generalized Admittance Matrix and, by using matrix transformations, the Generalized Scattering Matrix (GSM) are obtained.

The antenna is characterized as a closed circuit, which is then described by its GSM; [S] parameters relate modes in the input waveguide and SM in the sphere. Antenna parameters as return losses, directivity, beam widths and aperture efficiency can be obtained from the calculated scattering parameters. A complete description of the method can be consulted at D. Ramaccia et al. (2013), J. Rubio et al. (2001), and J. M. Gil et al. (2006).

3. Reduced Size Conical Horn Antennas Based on B.O.R

A horn with a wide flare angle can be an option to shorten the length of a standard conical horn. To correct the phase distortion that is produced at the aperture, a lens or inner dielectric or metamaterial can be used. In this way, physically small and compact antennas at millimeter and sub-millimeter wavelengths can be designed to be used in multiple applications like radar, transceivers and material characterization. The phase correcting lens has a focusing purpose trying to generate a plane-phase front at the aperture of the horn; this is traditionally obtained by means of a hyperbolic surface inner to the horn and plane at the aperture (convex-plane lens). The focusing effect transforms a spherical wave into a plane one; this is easily demonstrated by optical geometric theory though, at the aperture of the horn, we have a near field instead of far field. Therefore, the ray-optics theory is just an approximation and the addition of some corrections may be adequate to improve the focusing of the lens and then, the performance of the antenna. A full wave analysis of the antenna,

as the method proposed in this paper, is the more reliable approach to obtain these corrections. On the other hand, a horn with a hyperbolic convex-plane lens has a limitation because the lens is completely inner to the conical horn so the optimal focal point could go outside of the horn. To avoid this obstacle, we can use a double-convex lens and optimize its thickness to achieve the enhancement of the parameters of the antenna under optimization. In Figure 2, a 45° flare angle horn, corrected by a convex-plane lens is shown. The profile of the lens is a hyperbolic surface inner to the horn. This antenna was studied in E. L. Holzman (2004) and we use it to check the current method. To apply our procedure, the geometry is surrounded by a sphere of radius $R = 4.1406$ cm. The mesh uses 22,400 triangles of order to 2, five circular waveguide modes at the input port and 160 SM at the output port. The Central Processing Unit time is around 7 seconds in a personal computer. These parameters of design are decided after a fine convergence study of the problem, both modal and relative to the density of the mesh.

The dielectric lens is made of Rexolite ($\epsilon_r = 2.548$ at 60 GHz). In Table 1, we compare our results with those predicted by E. L. Holzman (2004), at two frequencies. The author admits in E. L. Holzman (2004) some discrepancies with measurements due to an insufficient mesh density. Notice that the length of this antenna is 8 wavelengths.

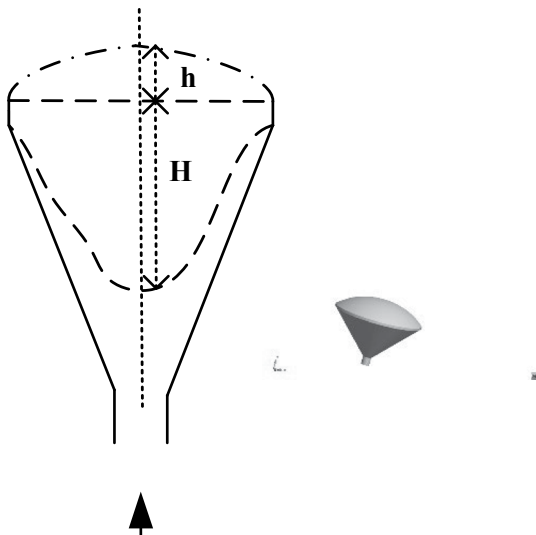


Figure 3. Double-convex lens inner to a conical 45° flare angle conical horn.

Table 2
Performance of a Shorted Double-Convex Lens Conical Horn

	D(dB)	XP(dB)	BWcop(°)	S ₁₁ (dB)
Plane-convex lens horn	22.7	-13.9	8.3	-14.3
Double-convex lens horn	26.2	-15.2	7.0	-24.9

We can improve the performance of this antenna replacing the hyperbolic convex-plane lens by a double convex lens and optimize the position of the focal point, that is, the thickness of the lens (Figure 3). As we mentioned, is important to notice that, when a hyperbolic lens is used inner to the horn, with the intention to correct the degradation of the phase diagram at the aperture due to a wide flare angle of the horn, the use of a plane hyperbolic lens may not be enough to reach an optimal performance of the antenna. That is due to the geometrical limitation inherent to the fact that the horn contains the hyperbolic lens. The variation of the focal point of the lens in order to change the phase diagram is then limited by the horn and this is an important limitation for the optimization process. The substitution of the hyperbolic convex-plane by a double-convex lens avoids this limitation and the optimization process can go farther and achieve an antenna presenting a better performance. This is the line of design we have adapted in this work to propose more compact and shortened antennas maintaining similar radiation parameters. Obviously, the addition of the double lens makes the horn a little larger but this disadvantage is not relevant.

We carry out the optimization of the horn at the central frequency (60 GHz). After a fine-tuning of the thickness of the lens, we founded the best geometry for the double-convex lens described at Figure 3. The optimized thickness of the lenses result $H = 2.867$ cm and $h = 0.57$ cm. The comparison of the optimized antenna, in relation to the horn described in Figure 2, is given in Table 2. An evident improvement can be noticed when a double-convex lens to focus the horn is employed.

The optimized horn presents a frequency behavior given in Figures 4 and 5. A pseudo-harmonic oscillation is noticed at the graphics due to reflections of the modes at the aperture. Despite of this, the parameters keep reasonable values along the whole band.

4. Additional Shortening of Conical Horn Antennas

Trying to get more compact and reduced-size antennas, we can shorten the length and keep the flare angle; obviously, the phase diagram at the aperture results deteriorated, and the performance of the antenna become poor. A complete study was reported in A. Rolland et al. (2010), by using an optimized profile of a hyperbolic plane-convex lens, inner to a conical horn with a 45° flare angle. The parameters obtained for the prototype are similar to those obtained with our procedure. The obtained profile results pseudo-harmonic and this design suffers of a poor frequency behavior, as the authors refer in the paper (A. Rolland et al., 2010). They report a fall of the directivity at the frequency of 62.5 GHz. It can be due to the pseudo-harmonic optimized profile of the lens, providing some non-desirable resonant effect. We present here a similar design based on a double-convex

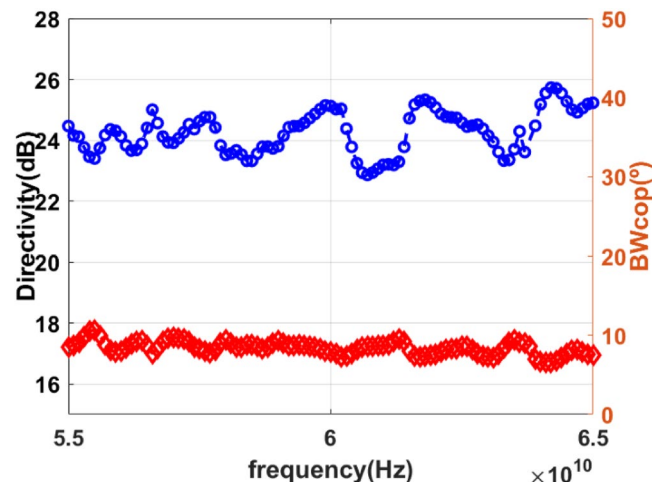


Figure 4. Directivity and Beam width co-polar versus frequency, for the antenna of Figure 3.

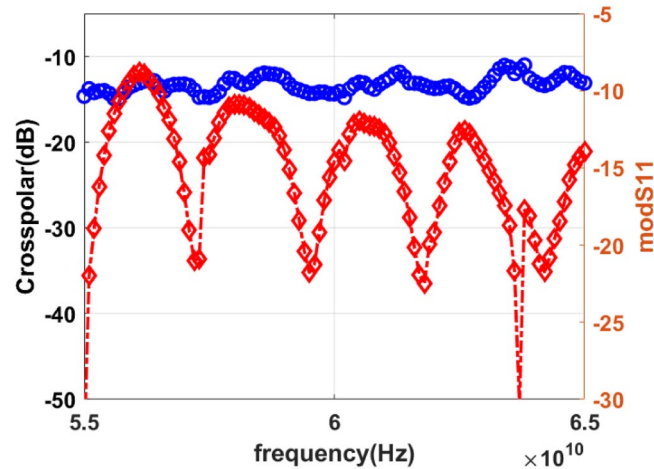


Figure 5. Peak cross-polar level and module of S11 versus frequency, for the antenna of Figure 3.

lens, with a hyperbolic profile, trying to improve its frequency behavior and achieving an antenna with a wider frequency band. The geometry is shown in Figure 6.

The optimized dimensions of the ultra-short horn are $L = 0.921$ cm (1.84λ); $T = 0.1$ cm; $d/2 = 0.17907$ cm; $D = 2$ cm (4λ); $H = 0.525$ cm and $h = 0.281$ cm, λ being the free-space wavelength. This prototype results around four times shorter than shown at Figure 2. If $h = 0$, that is, by using a plane hyperbolic lens ($\epsilon_r = 2.548$), at 60 GHz, the parameters of the antenna result: $D = 15.6$ dB; $XP = -11.7$ dB; $BW_{cop} = 28.1^\circ$; $|S_{11}| = -15.0$ dB. By adding the outer lens ($h = 0.281$ cm), the performance of the antenna results significantly improved:

$$D = 19.0 \text{ dB}; XP = -13.0 \text{ dB}; BW_{cop} = 18.7^\circ; |S_{11}| = -32.8 \text{ dB}$$

The frequency behavior is shown in Figures 7 and 8. In Figure 7, we can see how the directivity presents a similar behavior as reported in A. Rolland et al. (2010), but our design avoids the downfall at the frequency of 62.5 GHz and follows a stable pattern. In Figure 8, the adaptation of the antenna is shown, presenting an excellent behavior along the band and a very low voltage standing wave ratio around the central frequency at 60 GHz.

By adding a dielectric core, the horn supports hybrid modes. The dielectric modifies the field on the aperture, affecting to the radiation pattern. Lower levels of cross polar peak are achieved, which can be useful in multi-antenna systems where a high discrimination between the two linear polarizations is mandatory. In Figure 9, we can see the section of the horn with four segments: the double-convex hyperbolic lens made of Rexolite ($\epsilon_4 = 2.548$); the dielectric core (ϵ_3), with a softened section at the throat in order to achieve a better matched input impedance; a dielectric support made of foam with a permittivity similar to the air ($\epsilon_2 = 1.04$),

and the circular waveguide with a permittivity equal to the air ($\epsilon_1 = 1$). The optimum gap between the dielectric core and the external layer of the horn is $g = 0.1$ cm. In Figure 10, we show the three separated segments and the completed horn. The disassembly of the antenna provides the manufacture of each segment separately by additive techniques. Some sections can be directly printed or, in case it would not be able to get a printing commercial material, print a structure with an effective permittivity of the same value that the dielectric we want to manufacture. Procedures for tailoring the effective permittivity of materials not available commercially, by using 3D-printing processes, have been described along several works, for instance (S. Zhang et al., 2016). Then, the horn is built after assembling the segments and metalizing the external layer.

After a parametric study of the permittivity of the segments, we founded like optimal solution the employment of Rexolite, for a given thickness ($H + h$) of the lens. The addition of the dielectric core needs a new parametric study which is shown in Figures 11 and 12.

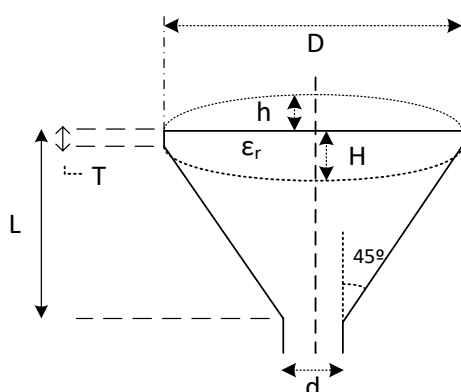


Figure 6. Ultra short double-convex lens conical horn.

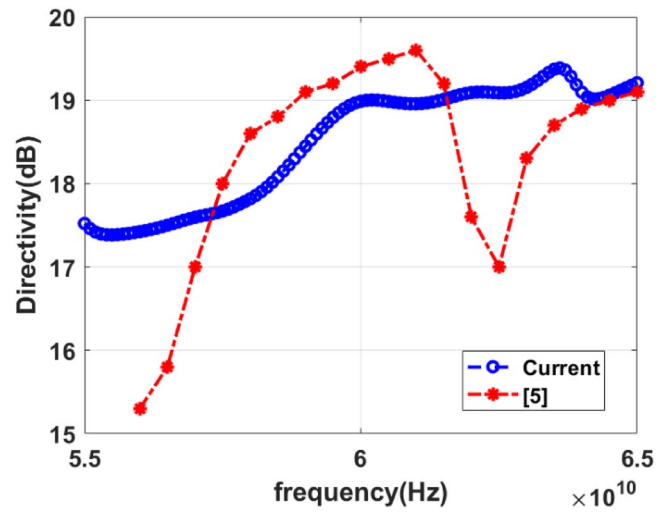


Figure 7. Directivity of the ultra-short double-convex lens conical horn versus frequency.

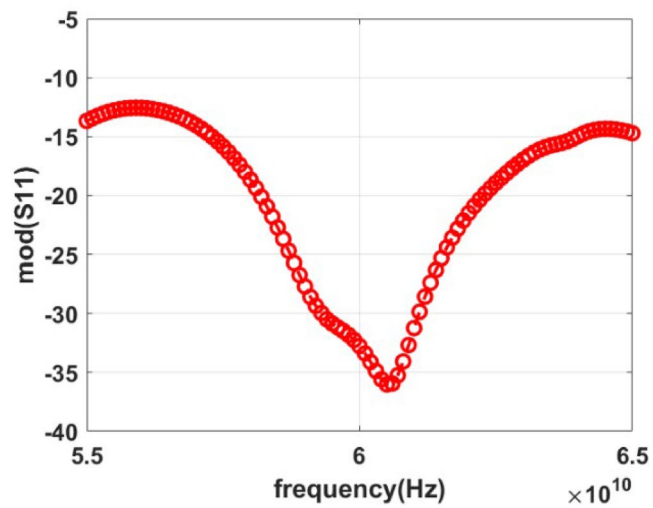


Figure 8. Module of S11 of the ultra-short double-convex lens conical horn versus frequency.

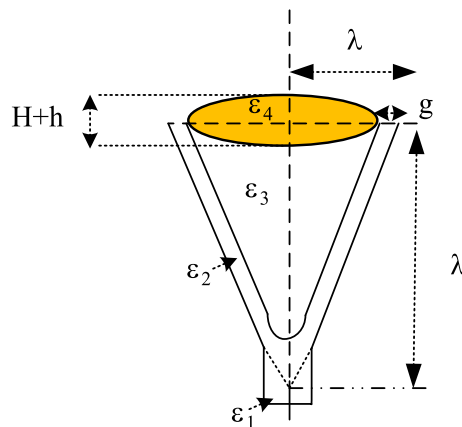


Figure 9. Ultra-short double-convex lens dielectric core horn.

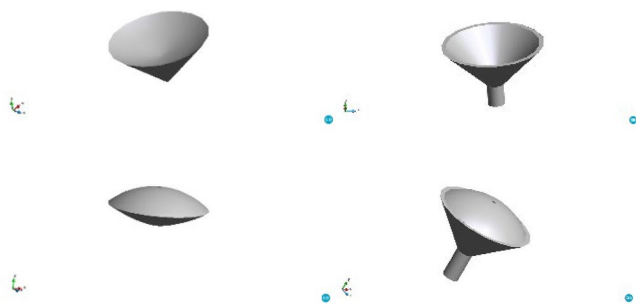


Figure 10. Segmented horn; from left to right and up to down: dielectric-core, foam support, double-convex lens and the assembled horn.

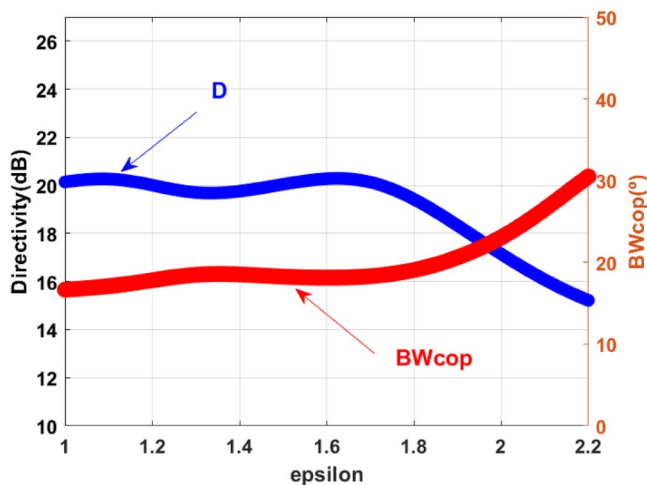


Figure 11. Parametric study of permittivity of the dielectric core (ϵ_3), relative to both, Directivity (D) and Beam width (BWcop), for the horn in Figure 9.

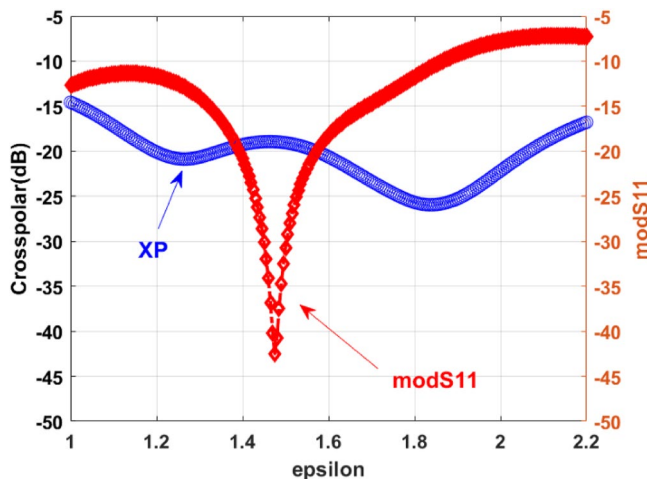


Figure 12. Parametric study of permittivity of the dielectric core (ϵ_3), relative to both, Peak cross-polar (XP) and module of S11 (modS11), for the horn in Figure 9.

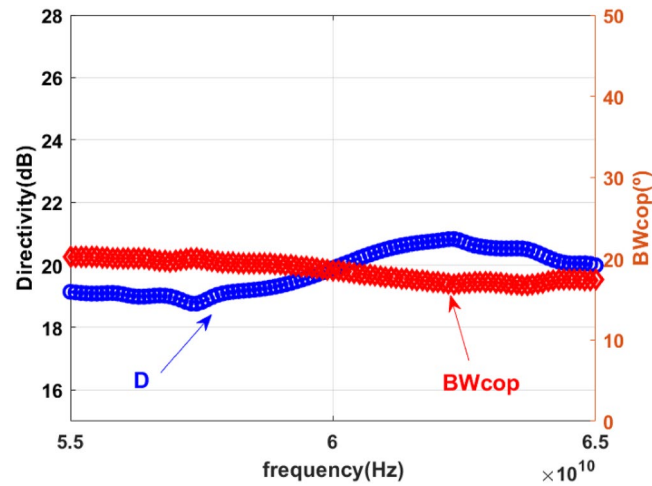


Figure 13. Directivity and Beam width co-polar versus the frequency, for the horn in Figure 9.

The optimal value of the permittivity is founded around $\epsilon_3 = 1.5$. The parameters of the antenna result:

$$D = 20.0 \text{ dB}; XP = -19.1 \text{ dB}; BW_{\text{cop}} = 18.3^\circ; |S_{11}| = -30.7 \text{ dB}$$

It is worth remembering that the previous performance is relative to a horn (Figure 9) with a length of almost only one wavelength.

After achieving an optimized design of the horn, it is important to explore the frequency behavior of the antenna. The performance of the antenna versus the frequency is shown at the Figure 13 (directivity and co-polar beam-width), and Figure 14 (peak cross-polar and module of S11).

It is interesting to point out the stable frequency behavior of the Directivity and the Beam width throughout the band (Figure 14). On the other side, it is worth noticing the extremely high level of matching around the central frequency of 60 GHz (Figure 15).

Finally, the radiation patterns of the ultra-short horn for three frequencies, 58 GHz, 60 GHz and 62 GHz, are shown at Figures 15a–15c. A reasonable stability of the patterns, within the band, is observed.

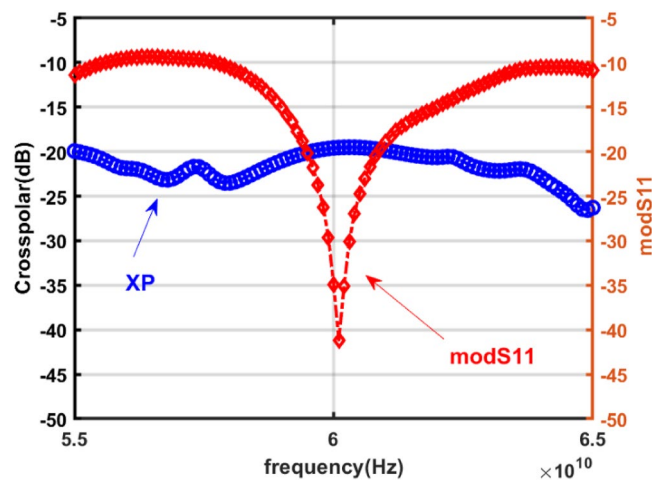


Figure 14. Peak cross-polar (XP) and module of S11 (modS11) versus frequency, for the horn in Figure 9.

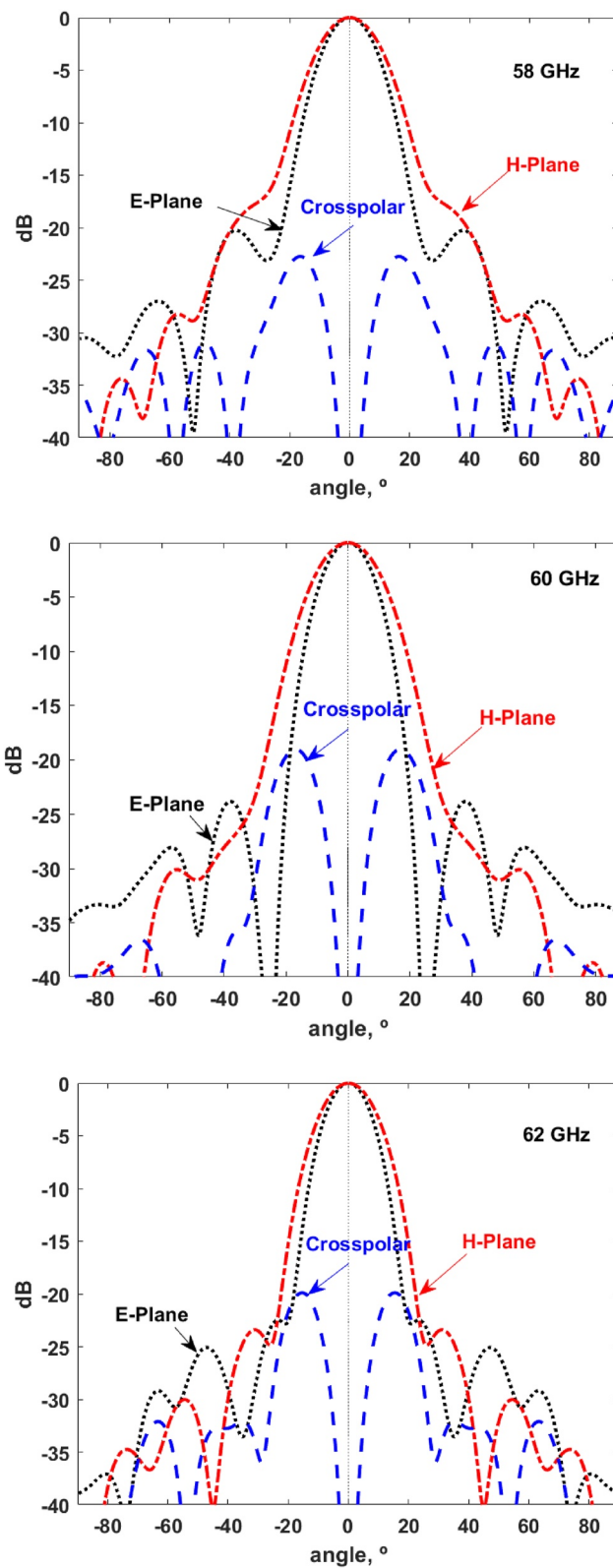


Figure 15. Radiation patterns of ultra-short double-convex lens horn of Figure 9. (---, H-Plane; E-Plane; ---- cross polar). (a) 58 GHz, (b) 60 GHz, (c) 62 GHz.

5. Conclusions

At millimeter wavelengths, ultra-high speed communications systems for wireless network demands compact and cheap small antennas with a reasonable performance. Reduced-size conical horn can play an interesting role whenever we can compensate the degradation of the phase distribution along the aperture that occurs when we change a long horn antenna by another shortened. This correction is achieved by means of the addition of lens, an optimization process and/or parametric studies. At this work, some improvements in the design of ultra-short horn antennas, loaded with dielectric cores and lenses, are suggested. It is notice worth the final horn prototype, with a shortened length of almost one wavelength and a very remarkable performance over a reasonable bandwidth ($D = 20.0$ dB; $XP = -19.1$ dB; $BW_{\text{cop}} = 18.3^\circ$; $|S_{11}| = -30.7$ dB). The constituent elements of the prototypes, dielectric core, supports and lenses, might be easily manufactured exporting the geometries to a 3D printer. After printing the diverse components, we can link them and metalize the external dielectric layer obtaining the final device.

Data Availability Statement

Data were not used, nor created for this research.

Acknowledgments

This work was partially supported by Ministerio de Ciencia e Innovación (MCIN/AEI/10.13039/501100011033/FEDER, UE) under project PID2021-122856NB-C22.

References

- Alibakhshikenari, M., Ali, E. M., Soruri, M., Dalarsson, M., Naser-Moghadasi, M., Virdee, B. S., et al. (2022). A comprehensive survey on antennas on-chip based on metamaterial, metasurface, and substrate integrated waveguide principles for millimeter-waves and terahertz integrated circuits and systems. *IEEE Access*, *10*, 3668–3692. <https://doi.org/10.1109/access.2021.3140156>
- Alibakhshikenari, M., Virdee, B. S., Azpilicueta, L., Naser-Moghadasi, M., Akinsolu, M. O., Hwang, C., et al. (2020). A comprehensive survey of “metamaterial transmission-line based antennas: Design, challenges, and applications. *IEEE Access*, *8*, 144778–144808. <https://doi.org/10.1109/access.2020.3013698>
- Al-Nuaimi, M. K. T., Hong, W., & Zhang, Y. (2014). Design of high-directivity compact-size conical horn lens antenna. *IEEE Antennas and Wireless Propagation Letters*, *13*, 467–470. <https://doi.org/10.1109/lawp.2013.2297519>
- Gil, J. M., Monge, J., Rubio, J., & Zapata, J. (2006). A CAD-oriented method to analyse and design radiating structures based on bodies of revolution by using finite elements and generalized scattering matrix. *IEEE Transactions on Antennas and Propagation*, *54*(3), 899–907. <https://doi.org/10.1109/tap.2005.863145>
- Holzman, E. L. (2004). A highly compact 60-GHz lens-corrected conical horn antenna. *IEEE Antennas and Wireless Propagation Letters*, *3*, 280–282. <https://doi.org/10.1109/lawp.2004.831082>
- Liu, K., Ge, Y., & Lin, C. (2019). Yuehe Ge and Chengxiu Lin, “A compact wideband high-gain metasurface-lens-corrected conical horn antenna”. *IEEE Antennas and Wireless Propagation Letters*, *18*(3), 457–461. <https://doi.org/10.1109/lawp.2019.2894037>
- Martínez-Fernández, J., Gil, J. M., & Zapata, J. (2007). Ultrawideband optimized profile monopole antenna by means of simulated annealing algorithm and the finite element method, member. *IEEE Transactions on Antennas and Propagation*, *55*(6), 1826–1832. <https://doi.org/10.1109/tap.2007.898593>
- Ramaccia, D., Scattone, F., Bilotti, F., & Toscano, A. (2013). Broadband compact horn antennas by using EPS-ENZ metamaterial lens. *IEEE Transactions on Antennas and Propagation*, *61*(6), 2929–2937. <https://doi.org/10.1109/tap.2013.2250235>
- Rolland, A., Ettorre, M., Drissi, M. H., Le Coq, L., & Sauleau, R. (2010). Optimization of reduced-size smooth-walled conical horns BoR-FDTD and genetic algorithm. *IEEE Transactions on Antennas and Propagation*, *58*(9), 3094–3100. <https://doi.org/10.1109/tap.2010.2052557>
- Rubio, J., Arroyo, J., & Zapata, J. (2001). SFELP-an efficient methodology for microwave circuit analysis. *IEEE Transactions on Microwave Theory and Techniques*, *49*(3), 509–516. <https://doi.org/10.1109/22.910555>
- Shaik, M., & Rama, T. (2013). Concave lens integrated conical horn at 60 GHz for energy efficient wireless applications. In *International conference on advances in computing, communications and informatics (ICACCI)*. Mysore.
- Wu, D., Feng, Z., & Zhuang, X. (2015). A novel focusing conical horn antenna loaded with dielectric. IEEE International Wireless Symposium.
- Zhang, S., Cadman, D., & Vardaxoglou, J. Y. C. (2018). Additively manufactured profiled conical horn antenna with dielectric loading. *IEEE Antennas and Wireless Propagation Letters*, *17*(11), 2128–2132. <https://doi.org/10.1109/lawp.2018.2871029>
- Zhang, S., Kumar, R., Pandey, S., Vardaxoglou, Y., Whittow, W., & Mitra, R. (2016). 3D-printed planar graded index lenses. *IET Microwaves, Antennas & Propagation*, *10*(13), 1411–1419. <https://doi.org/10.1049/iet-map.2016.0013>